Aluminum gallium nitride short-period superlattic s doped with magnesium

A. Saxler[a] and W. C. Mitchel
Air Force Research Laboratory, Materials and Manufacturing Directorate, AFRL/MLPO, Wright–Patterson AFB, Ohio 45433-7707

P. Kung and M. Razeghi
Center for Quantum Devices, Department of Electrical and Computer Engineering, Northwestern University, Evanston, Illinois 60208

Short-period superlattices consisting of alternating layers of GaN:Mg and AlGaN:Mg were grown by low-pressure organometallic vapor phase epitaxy. The electrical properties of these superlattices were measured as a function of temperature and compared to conventional AlGaN:Mg layers. It is shown that the optical absorption edge can be shifted to shorter wavelengths while lowering the acceptor ionization energy by using short-period superlattice structures instead of bulk-like AlGaN:Mg. © *1999 American Institute of Physics.* [S0003-6951(99)03714-6]

Many applications exist for the III nitrides in high-power and high-temperature electronics,[1] solar-blind ultraviolet photodetectors,[2] and blue and ultraviolet light-emitting and laser diodes,[3] but materials issues still dominate. One of the remaining issues is the p-type doping of the III nitrides, especially AlGaN with high aluminum mole fractions, partially because of the relatively deep acceptors.[4–8] We have previously reported III-nitride growth,[9–12] characterization,[13,14] and photodetectors.[15,16] In this letter, we present the p-type doping of AlGaN short-period superlattices (SPSL's) with the motivation of reducing acceptor ionization energies, and we compare this technique to the doping of single AlGaN layers. Also, superlattices of AlGaN have been used for reducing cracking in the confinement layers of III-nitride lasers,[17] so it is useful to understand their electrical properties. We expect the improved p-type doping through the use of AlGaN SPSLs to enhance device performance by providing better optical and electrical confinement or shorter-wavelength operation because of the increased effective energy gap of the SPSL without increasing the device resistance.

The III-nitride layers were grown in a horizontal low-pressure (10 mbar) organometallic vapor phase epitaxy reactor manufactured by AIXTRON (AIX200/4 HT). The gallium, aluminum, nitrogen, and magnesium sources were triethylgallium (TEGa), trimethylaluminum (TMAl), ammonia (NH_3), and biscyclopentadienylmagnesium (Cp_2Mg), respectively.

A 50 nm thick, high-temperature (1100 °C) AlN nucleation layer was deposited on (0001) Al_2O_3 substrates prior to the deposition of an AlGaN layer or superlattice at 1050 °C with a total thickness of 0.7 μm. Following the growth, the samples were annealed in the reactor at 900 °C in nitrogen for 10 min to remove the hydrogen passivation of the acceptors. Table I shows the structures of the SPSLs including the layer thicknesses and aluminum concentrations. The cutoff wavelengths of the SPSLs studied are also shown in Table I. (The arbitrarily chosen $\lambda_{50\%}$ is defined as the wavelength at

which half of the light is transmitted through the film. This wavelength falls on the steep slope of the transmission curve and corresponds to about 10^4 cm^{-1} for these 0.7 μm thick samples.)

Figure 1 is a diagram of the valence band (VB) of a SPSL, drawn without any bandbending. $E_{A,GaN}$ and $E_{A,AlGaN}$ are the acceptor ionization energies in GaN and AlGaN, respectively. ΔE_{VB} is the valence-band offset, and ΔE_{SL} is the offset of the bottom of the first miniband of the SPSL from the valence band of GaN. For true superlattice behavior, the barriers must be very thin so the wave function can penetrate in spite of the large effective hole mass. The positions of the minibands can be simply calculated,[18] but the effective masses and valence-band offsets are not yet well known for the AlGaN system.[19–21] Assuming ranges for the electron effective mass to be $0.18-0.23m_0$, the hole effective mass to be $0.54-2.2m_0$, the valence-band offset to be 18%–50%, and the bowing parameter 0–1 eV; the minimum and maximum wavelength shifts of the absorption edge for these values are recorded in Table I. These values were in reasonable agreement with the experiment as seen in Table I. Using the diagram, the acceptor ionization energy is given by one of the following equations:

$$E_{A,SPSL} = E_{A,AlGaN} + \Delta E_{SL} - \Delta E_{VB}, \qquad (1)$$

$$E_{A,SPSL} = E_{A,GaN} + \Delta E_{SL}. \qquad (2)$$

If each constituent layer is p type, the smaller of Eqs. (1) and (2) will be the initial ionization energy, because the effectively shallower acceptors will be the first to be ionized ei-

TABLE I. Sample data including superlattice layer thicknesses, composition of the $Al_xGa_{1-x}N$ layer, cutoff wavelengths, and acceptor ionization energies.

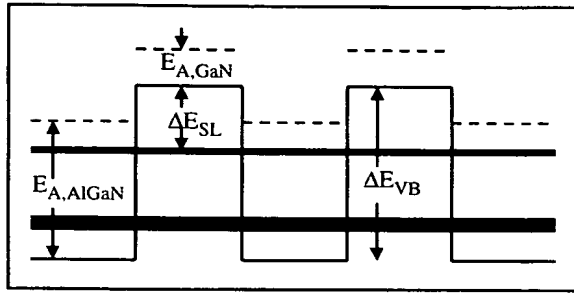| Sample	t_{GaN} (Å)	t_{AlGaN} (Å)	x	λ_{50} (nm)	$\Delta\lambda_{meas}$ (nm)	$\Delta\lambda_{min\,calc}$ (nm)	$\Delta\lambda_{max\,calc}$ (nm)	$E_{A\,meas}$ (meV)
813	23	23	0.30	350	17	13	22	124
821	39	8	0.30	361	6	5	9	116
824	8	17	0.45	326	41	40	63	268
825	8	9	0.45	335	32	35	53	240

[a]Electronic mail: adam.saxler@afrl.af.mil

FIG. 1. Schematic diagram of the valence band of a superlattice. Shaded lines are the minibands of the superlattice. Dashed lines are the dopant levels in their host material.

ther from the AlGaN [Eq. (1)] or from the GaN [Eq. (2)]. However, if the AlGaN layer were fully compensated, as is likely in very high aluminum content layers,[7] Eq. (2) would be relevant since there would not be any non-ionized acceptors in the AlGaN layer. A very wide range of values can be obtained for these equations, including negative values for Eq. (1), depending on the material constants used.

X-ray diffraction curves were obtained using a Philips high resolution diffractometer (HRD) system with a mono-chromator utilizing four (220) Ge reflections. Figure 2 shows the $\omega/2\theta$ curve of a Mg-doped GaN/AlGaN SPSL. In addition to the main peak, both the AlN buffer layer peak and the -1 superlattice peak are visible. The presence of the super-lattice peak confirms that there is indeed a superlattice instead of a mixed alloy. The superlattice period calculated from the peak positions agrees with the expected thickness based on the growth rates of the constituent layers of the SPSL. The rocking curve linewidths of the main superlattice peaks were relatively narrow (100–200 arc s) for all of the samples, indicating good structural quality.

UV–visible transmission curves were obtained using a dual-beam spectrometer with a sapphire substrate in the reference beam. Figure 3 shows the optical transmission curve for a SPSL compared with curves for its constituent GaN:Mg and AlGaN:Mg layers. As expected, the onset of the absorption edge of the SPSL is clearly shifted to a shorter wavelength than GaN. Once the absorption edge is reached, the bulk-like binary and ternary films quickly absorb all of the incident light, within the limit of the background noise. This contrasts with the transmission curve of the SPSL, which has a small peak below the initial absorption edge. This is consistent with absorption between the minibands of the SPSL,
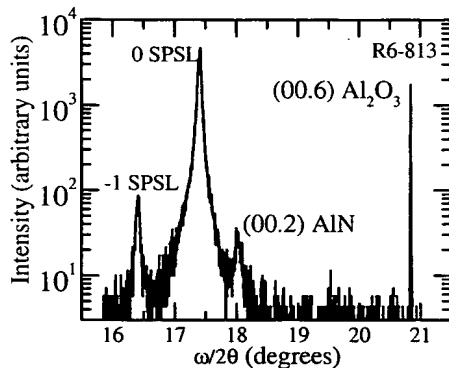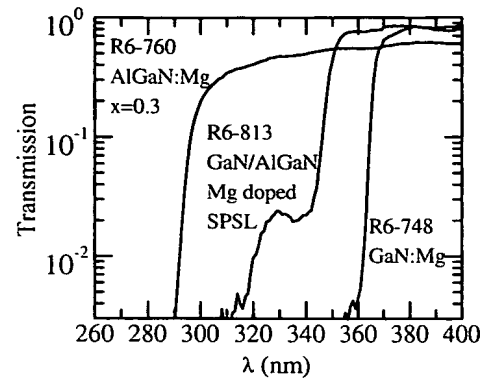

FIG. 3. Optical transmission of III-nitride films.

with the initial dip in transmission corresponding to the transition between the lowest-energy minibands in the conduction and valence bands. The small peak in transmission would then correspond to transition energies above these minibands.

Figure 4 shows the resistivity as a function of temperature for a magnesium-doped GaN/AlGaN SPSL and its constituent layers. Temperature-dependent Hall-effect and resistivity measurements were taken using Ni/Au contacts in the van der Pauw configuration in nitrogen or helium gas at atmospheric pressure. The hole concentration could not always be obtained because the noise was often larger than the Hall voltage, largely because of the low hole mobilities that were, typically, less than 10 cm^2/V s. Assuming the mobility is comparatively temperature independent, the acceptor ionization energy was extracted by assuming resistivity is inversely proportional to $T^{3/2}e^{-E_A/kT}$, where T is the absolute temperature, E_A is the acceptor ionization energy, and k is the Boltzmann constant. Only the steepest part of the curve was used in the fit, to exclude hopping conduction at the lowest temperatures and both saturation and irreversible changes which sometimes occurred at the highest temperatures.

The data from fits for several samples are summarized both in Table I and in Fig. 5, which plots the acceptor ionization energy as a function of the cutoff wavelength at

FIG. 2. X-ray diffraction $\omega/2\theta$ curve of a magnesium-doped GaN/AlGaN SPSL.
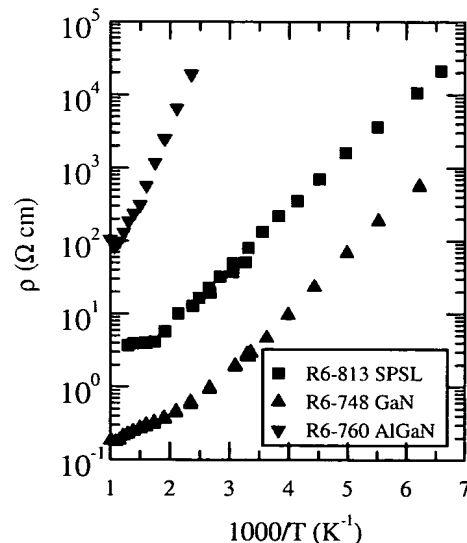

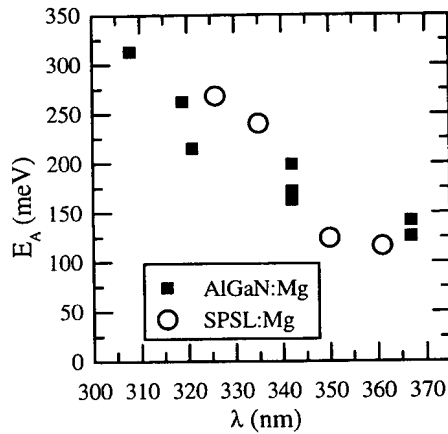FIG. 4. Temperature-dependent resistivity of III-nitride films.

FIG. 5. Acceptor ionization energies as a function of optical absorption edge (50% transmission) of bulk-like AlGaN:Mg compared with Mg-doped GaN/AlGaN short-period superlattices.

which 50% of the light is transmitted. In Fig. 5, the ionization energies of the bulk-like AlGaN and SPSLs can be easily compared. These initial data points show that it is possible to lower the acceptor ionization energy for a given cutoff wavelength by using this doping technique. The increased ionization energy for the higher aluminum containing SPSLs could be due to a larger number of compensating donors changing the position where the Fermi level is pinned.

Short-period superlattices consisting of alternating layers of GaN:Mg and AlGaN:Mg were grown by low-pressure organometallic vapor phase epitaxy. The electrical properties of these superlattices were measured as a function of temperature and compared to conventional AlGaN:Mg layers. It is shown that the optical absorption edge can be shifted to shorter wavelengths while lowering the acceptor ionization energy by using short-period superlattice structures instead of bulk-like AlGaN:Mg. Since the hole effective mass is much larger than the electron effective mass, and the conduction-band offset is larger than that of the valence band, most of the wavelength shift in the p-type SPSL will be due to the energy shift in the conduction band. This should be beneficial for most optoelectronic devices based

on this material. These initial results are very promising, and should encourage more detailed experimental and theoretical work, including application to devices.

[1] O. Aktas, Z. F. Fan, S. N. Mohammed, A. E. Botchkarev, and H. Morkoç, Appl. Phys. Lett. **69**, 3872 (1996).

[2] M. Razeghi and A. Rogalski, J. Appl. Phys. **79**, 7433 (1996).

[3] S. Nakamura, M. Seno, S. Nagahama, N. Iwasa, T. Yamada, T. Matsushita, Y. Sugimoto, and H. Kiyoku, Appl. Phys. Lett. **69**, 4056 (1996).

[4] M. Stutzmann, O. Ambacher, A. Cros, M. S. Brandt, H. Angerer, R. Dimitrov, N. Reinacher, T. Metzger, R. Höpler, D, Brunner, F. Freudenberg, R. Handschuh, and Ch. Deger, Mater. Sci. Eng., B **50**, 212 (1997).

[5] A. Saxler, *Exploration of LP-MOCVD Grown III-Nitrides on Various Substrates* (Northwestern University, Evanston, IL, 1998), pp. 154–163.

[6] T. Tanaka, A. Watanabe, H. Amano, Y. Kobayashi, I. Akasaki, S. Yamazaki, and M. Koike, Appl. Phys. Lett. **65**, 593 (1994).

[7] C. Stampfl and C. Van de Walle, Appl. Phys. Lett. **72**, 459 (1998).

[8] I. Akasaki and H. Amano, Jpn. J. Appl. Phys., Part 1 **36**, 5393 (1997).

[9] A. Saxler, D. Walker, P. Kung, X. Zhang, M. Razeghi, J. Solomon, W. C. Mitchel, and H. R. Vydyanath, Appl. Phys. Lett. **71**, 3272 (1997).

[10] A. Saxler, P. Kung, C. J. Sun, E. Bigan, and M. Razeghi, Appl. Phys. Lett. **64**, 339 (1994).

[11] P. Kung, A. Saxler, X. Zhang, D. Walker, T. C. Wang, I. Ferguson, and M. Razeghi, Appl. Phys. Lett. **66**, 2958 (1995).

[12] P. Kung, A. Saxler, X. Zhang, D. Walker, R. Lavado, and M. Razeghi, Appl. Phys. Lett. **69**, 2116 (1996).

[13] X. Zhang, P. Kung, D. Walker, A. Saxler, and M. Razeghi, Mater. Res. Soc. Symp. Proc. **395**, 625 (1996).

[14] A. Saxler, M. A. Capano, W. C. Mitchel, P. Kung, X. Zhang, D. Walker, and M. Razeghi, Mater. Res. Soc. Symp. Proc. **449**, 477 (1997).

[15] D. Walker, A. Saxler, P. Kung, X. Zhang, M. Hamilton, J. Diaz, and M. Razeghi, Appl. Phys. Lett. **72**, 3303 (1998).

[16] D. Walker, X. Zhang, A. Saxler, P. Kung, J. Xu, and M. Razeghi, Appl. Phys. Lett. **70**, 949 (1997).

[17] S. Nakamura, IEEE J. Sel. Top. Quantum Electron. **4**, 483 (1998).

[18] G. Bastard, *Wave Mechanics Applied to Semiconductor Heterostructures* (Halsted Press, New York, 1988), p. 21.

[19] S. Elhamri, R. S. Newrock, D. B. Mast, M. Ahoujja, W. C. Mitchel, J. M. Redwing, M. A. Tischler, and J. S. Flynn, Phys. Rev. B **57**, 1374 (1998).

[20] J. S. Im, A. Moritz, F. Steuber, V. Härle, F. Scolz, and A. Hangleiter, Appl. Phys. Lett. **70**, 631 (1997).

[21] S. W. King, C. Ronning, R. F. Davis, M. C. Benjamin, and R. J. Nemanich, J. Appl. Phys. **84**, 2086 (1998).